

Underground renewal time and mixing of the main mineral waters of Tunisia: A multi-tracer study

Philippe Jean-Baptiste, Elise Fourré, Elyès Gaubi, B. Minster, Luc Aquilina, Thierry Labasque, J.L. Michelot, Marc Massault, Abdallah Ben Mammou

► **To cite this version:**

Philippe Jean-Baptiste, Elise Fourré, Elyès Gaubi, B. Minster, Luc Aquilina, et al.. Underground renewal time and mixing of the main mineral waters of Tunisia: A multi-tracer study. *Applied Geochemistry*, Elsevier, 2017, 85 (Part A), pp.10-18. <10.1016/j.apgeochem.2017.08.006>. <insu-01578508>

HAL Id: insu-01578508

<https://hal-insu.archives-ouvertes.fr/insu-01578508>

Submitted on 29 Aug 2017

HAL is a multi-disciplinary open access archive for the deposit and dissemination of scientific research documents, whether they are published or not. The documents may come from teaching and research institutions in France or abroad, or from public or private research centers.

L'archive ouverte pluridisciplinaire **HAL**, est destinée au dépôt et à la diffusion de documents scientifiques de niveau recherche, publiés ou non, émanant des établissements d'enseignement et de recherche français ou étrangers, des laboratoires publics ou privés.

30 1. Introduction

31

32 The rapid increase in bottled mineral groundwater production in Tunisia needed to
33 meet consumer demand (110 millions bottles in 1995 and 1.04 billion bottles in 2015
34 – Office du thermalisme at *www.thermalisme.nat.tn*) raises the question of the long-
35 term sustainability of this economic sector.

36 Renewal time of groundwater, which is clearly related to the ratio of the storage
37 volume to the recharge rate, is an important notion regarding vulnerability and
38 sustainability of groundwater resources. Numerical models of groundwater flow can
39 describe accurately the hydrodynamic functioning of a given aquifer, and therefore
40 can give stakeholders and the mineral water industry management important
41 indications to prevent pollution and/or overexploitation of the water resource.
42 However, they require detailed information (e.g. boundary conditions, hydraulic
43 conductivity, porosity, etc...) which are usually not available. As an alternative, the
44 analysis of atmospheric transient tracer concentrations in groundwaters can provide
45 important basic information on their residence time and mixing.

46 As a development arising from tritium, which can be used as a transient tracer as
47 a result of ^3H injection into the atmosphere from the atmospheric testing of nuclear
48 devices in the 50's and early 60's, the ^3H - ^3He dating method offers a direct measure
49 for the time since groundwater had its last gas exchange with the atmosphere. The
50 ^3H - ^3He pair is of particular interest because tritium and its daughter helium-3 are
51 assumed to be fully conservative tracers, and also because the ^3H - ^3He radioactive
52 clock only relies on the in-situ $^3\text{H}/^3\text{He}$ ratio. Hence, it is independent of the history of
53 tritium input to the aquifer (Schlosser et al., 1988, 1989; Poreda et al., 1988;
54 Solomon et al., 1991, 1993; Stute et al., 1997).

55 Like tritium, ^{14}C was also a by-product of atmospheric nuclear tests. Hence, the
56 resultant transient spike in atmospheric $^{14}\text{CO}_2$ can also be used as a transient tracer
57 (Stewart, 2012; Baudron et al., 2013).

58 The CFCs and SF_6 methods are based on the direct comparison of the
59 groundwater tracer concentration with the concentration of these tracers in the
60 atmosphere, and hence in groundwater recharge. Because their atmospheric
61 concentration has changed through time, this provides the basis for travel time
62 determination (Thompson and Hayes, 1979; Cook and Solomon, 1995; Busenberg
63 and Plummer, 1992, 2000; Goody et al., 2006; Darling et al., 2012).

64 Each tracer has its own atmospheric input function and each tracer method relies
65 on its own specific set of assumptions and caveats. There are significant differences
66 in the reliability of the derived tracer ages. Some caveats are the result of
67 hydrogeology. For CFCs and ^{14}C additional uncertainties of the infiltration conditions
68 influence the resulting ages. Therefore the combination of several tracer methods in
69 parallel is highly preferable to the use of a single method (Szabo et al., 1996; Beyerle
70 et al., 1999; Plummer et al., 2001; Corcho Alvarado et al., 2005, 2007; Massmann et
71 al., 2008; Solomon et al., 2010; Mayer et al., 2014; Kralik et al., 2014; Delbart et al.,
72 2014; Battle-Aguilar et al., 2017). Ideally measured tracer concentrations in a
73 groundwater can be matched simply to a particular year of recharge. However, this
74 requires that the groundwater moves as a result of simple piston flow, that is along
75 parallel flowlines from recharge to discharge. In reality, groundwaters are often a
76 mixture of water of different ages due to the complexity of the hydrogeological
77 network and/or the internal structure of the aquifer. One basic way of resolving flow
78 processes is to plot one tracer versus another (see for instance Figure 3 in Darling et
79 al., 2012). On these plots, simple piston flow and binary mixing between young

80 recharge waters and old tracer-free waters are opposite extremes of groundwater
81 behaviour. In most cases however, groundwater flow may be more complicated and
82 one must test a variety of modeled reservoirs connected to each other serially or in
83 parallel with or without dead volumes, cross flow in between or bypass flow (see
84 Ozyurt and Bayari, 2003 and references therein).

85 Here we report the application of such a multi-tracer approach to a suite of
86 mineral waters of Northern and Central Tunisia among the main commercial brands.
87 The region is characterized by a semi-arid climate with mild wet winters and hot dry
88 summers (monthly average temperatures vary from $10\pm 1^{\circ}\text{C}$ in January to $28\pm 2^{\circ}\text{C}$ in
89 August), and relatively low annual rainfall in the range 300 mm – 600 mm. For this
90 study, we selected eleven bottled water production sites (Table 1), exploiting local
91 aquifers nested in karstified limestone and/or sandstone formations (see Appendix
92 A). Very little is known by the operators concerning the actual extent of their mineral
93 groundwater resources and the sustainability of their business. Comparison of
94 mineral water withdrawal rates and recharge rates estimated from precipitation
95 figures and catchments' surface area shows that the rate of water withdrawal
96 exceeds the present-day recharge rate. This overexploitation of the local mineral
97 groundwater reservoirs may have serious implications in term of water quality and
98 economic consequences for the mineral water industry. Note that the issue of
99 groundwater overexploitation in Tunisia is not restricted to mineral waters: Tunisia,
100 being a semi-arid to arid country, is facing water shortage of increasing severity as a
101 result of population growth, rising living standards and increasing water consumption
102 by the agricultural sector (Frija et al., 2014)

103 The present work aims at exploring the potential of the selected suite of transient
104 tracers (tritium/helium-3, SF₆, CFCs and radiocarbon) to gain insight into the
105 hydrogeological characterization of these different water reservoirs.

106

107 **1. Sample collection and analytical methods**

108

109 The sampled sites are shown in Fig. 1, and their main characteristics (climatic
110 conditions, elevation, ...) are summarized in Table 1. Groundwaters were analyzed
111 for ¹⁸O/¹⁶O, D/H, ³H, ³He, ⁴He, ²⁰Ne, CFCs (F-11, F-12, F-113), SF₆ and ¹⁴C. Apart
112 from Marwa-2009 which shows a high neon supersaturation (see below), the
113 samples were taken at the water extraction point (at the well-head for pumped waters
114 and at the capture point for natural springs) so that contact of the water with the
115 atmosphere can be excluded. With the exception of a few tritium/helium and ¹⁴C
116 samples taken in October 2009, all the water samples were collected in
117 September/October 2010.

118 CFCs and SF₆ samples were collected in air tight stainless steel cells of 30 and
119 500 ml respectively and were analyzed at the University of Rennes (Labasque et al.,
120 2006; Ayraud et al., 2008). The CFC and SF₆ concentrations were determined by
121 Purge and Trap (PT) extraction and analysed with a gas chromatograph equipped
122 with an electron capture detector (GC/ECD). The uncertainty is 3% for water
123 equilibrated with the present-day atmosphere for CFC and 5% for SF₆ (see Table 2).

124 Noble gas samples (He, Ne) were collected using standard refrigeration grade
125 3/8" copper tubes equipped with metal clamps at both ends. ³H samples were
126 collected in 500 ml pyrex bottle, baked at 75°C and pre-filled with argon. The tritium
127 and noble gas isotopic analyses (³He, ⁴He, ²⁰Ne) were carried out at LSCE (CEA-

128 Saclay) with a MAP-215 mass spectrometer using standard procedures. Helium and
129 neon dissolved in the water samples were first extracted under vacuum into sealed
130 glass tubes. The accuracy is $\pm 0.8\%$ for helium and neon concentrations, and $\pm 0.4\%$
131 for the $^3\text{He}/^4\text{He}$ ratio. Water for tritium determination was degassed and stored during
132 9 to 12 months to allow for ^3He ingrowth. Uncertainty on tritium determination is given
133 in Table 2. Technical details concerning laboratory treatments and analytical
134 methods are available in Jean-Baptiste et al., 1992, 2010.

135 Carbon-14 samples were taken in 500 ml stainless steel cells and analyzed by
136 accelerator mass spectrometry at the French Radiocarbon National facility (CEA-
137 Saclay), with an accuracy between ± 0.1 pmC and ± 0.2 pmC (see Table 2). Delta ^{13}C
138 was measured by IRMS at Paris-Sud University, with an accuracy of ± 0.1 ‰.

139 Water for stable isotope analysis was collected in 15 ml glass bottles. Deuterium
140 and oxygen-18 were analysed at LSCE (CEA-Saclay) by laser spectrometry.
141 Uncertainties are ± 0.15 ‰ and ± 0.7 ‰ for oxygen-18 and deuterium respectively.

142

143 **3. Results**

144

145 Analytical results are shown in Table 2 . Stable isotopes are between -50.5‰
146 and -31.6‰ for D/H and between -7.66 and -5.10 for $^{18}\text{O}/^{16}\text{O}$, respectively. The
147 lowest values correspond to the El Kef region and reflect the altitude effect of this
148 more elevated area (altitude > 850 m – see Table 1) on the water isotopes
149 composition of rainwaters (Ambach et al., 1968; Siegenthaler and Oeschger, 1980).
150 The results are consistent with precipitation isotopic data for northern and central
151 Tunisia represented by the Tunis and Sfax Local Meteoric Water Lines (Fig. 2),

152 indicating that the rainfall contributing to the recharge did not undergo any significant
153 evaporation before infiltration.

154 All waters are tagged to various degree with environmental tracers of the post-
155 1950 era (Table 1). In spite of this, all carbon-14 values (range : 2.2 to 68.7 pmC) are
156 well below the natural modern pre-nuclear value of 100 pmC. The lowest value
157 corresponds to the carbo-gaseous waters of Ain Garci ($[\text{HCO}_3] = 19.8 \text{ mmol/l}$), clearly
158 showing the influence of the ^{14}C dilution by dead carbon on the ^{14}C result. $\delta^{13}\text{C}_{\text{TDC}}$
159 data were used to correct measured ^{14}C activities for dead carbon dilution due to
160 bicarbonate formation during the reaction between carbonic acid originating from soil
161 CO_2 and carbonate minerals (Clark and Fritz, 1997; Han and Plummer, 2016). For
162 this correction, the initial $\delta^{13}\text{C}$ value in groundwater recharge prior to leaving the
163 water-soil gas interaction zone is set to -12 ‰ (Clark and Fritz, 1997; Fourré et al.,
164 2011) and the $\delta^{13}\text{C}$ of the marine carbonate limestone formations (see Appendix A) is
165 assumed to be 0 ‰ (Clark and Fritz, 1997).

166 Neon excess relative to solubility equilibrium at the recharge temperature and
167 elevation ranges from -0.4% to 50.1% (mean value of 21.4%), with the exception of
168 Marwa which show a very large excess in 2009 (230%). This large anomaly, which is
169 confirmed by the analysis of a backup sample, is not seen in 2010 (26.6%). The most
170 probable explanation for the difference between 2009 and 2010 is the sampling
171 location : inside the bottling building in 2009 and at the well head in 2010. The neon
172 data are used to correct all tracer gas concentrations (^3He , ^4He , CFCs and SF_6) for
173 excess air (Aeschbach-Hertig et al., 1999) prior to age calculations and tracer
174 comparisons. In addition, all tracer concentrations are normalized to sea-level
175 pressure and a common temperature of 15°C to allow the comparison of all sites.

176 CFCs and SF₆ ages were determined from the direct comparison of the
177 groundwater tracer concentration with the time-dependent concentration of the tracer
178 in the groundwater recharge.

179 The ³H/³He age τ is defined as $\tau = \lambda^{-1} \ln(1 + ^3\text{He}_{\text{tri}}/^3\text{H})$, where λ is the decay
180 constant of tritium and ³H the measured tritium concentration. It is usually expressed
181 in tritium units (TU) : 1 TU corresponds to a ³H/H ratio of 10⁻¹⁸. ³He_{tri} is the fraction of
182 the total ³He that is produced by ³H decay, i.e. the difference between the measured
183 concentration ³He_{meas} and the concentrations of other ³He components : ³He_{atm} of
184 atmospheric origin, and ³He_{ter}, the terrigenic component : ³He_{tri} = (³He_{meas} - ³He_{atm} -
185 ³He_{ter}). ³He_{atm} and ³He_{ter} are deduced from the measured concentrations of helium
186 and neon. A terrigenic ratio ³He_{ter}/⁴He_{ter} of 2×10⁻⁸ typical isotope ratio for radiogenic
187 helium production in rocks was used, according to the work of Fourré et al. 2011
188 which shows the absence of mantle helium in the studied area (except for Ain Garci –
189 see below). Note that ³He_{ter} is very small, therefore ³He_{tri} is relatively insensitive to the
190 value of this terrigenic ³He/⁴He ratio.

191 Tracer ages are reported in Table 2 and Figure 3. (Fig. 3). SF₆ ages are younger
192 and F-11 ages older than ³H/³He, F-12 and F-113 ages, possibly due to in-situ
193 terrigenic SF₆ production and F-11 breakdown (see section 4 below). For Ain Garci,
194 ³H-³He dating was problematic due to the presence of mantle ³He
195 (³He/⁴He = 2.4 × Ra – see Fourré et al., 2011). ³H/³He, F-12 and F-113 ages range
196 from 10 to 58 years but tracer ages show substantial discrepancies. Age calculations
197 assume that groundwater moves along independent flowlines analogous to pipes
198 (piston flow). However, tracer-tracer plots (see section 4 below) indicate that the
199 groundwaters are a mixture of modern waters withwith older (tracer-free) waters.
200 Therefore, the piston flow conditions are not valid here and under these conditions it

201 is not possible to assign ages to tracer concentrations. Therefore tracer ages
202 reported here are not true ages but “apparent” ages (Suckow, 2014). Actual tracer
203 concentrations are modified by this mixing which, in turn, variously affects tracer
204 ages, thus explaining the substantial discrepancies among tracers.

205

206 **4. Discussion**

207

208 Figure 4a displays the mean annual atmospheric concentrations of CFCs, SF₆
209 and ¹⁴C as a function of time for the northern hemisphere. For tritium, the past history
210 of its concentration in precipitation in Tunisia was constructed using all historical
211 measurements from Central Mediterranean stations in the IAEA Global Network of
212 Isotopes in Precipitation database (at <https://nucleus.iaea.org/wiser/gnip.php>),
213 including the times-series of tritium in rainwater for Tunis and Sfax (Fig. 4b). Tunis
214 data agree with Central Mediterranean IAEA stations between 1970-1980 and then
215 seems to be overestimated, possibly due to data quality problems (some
216 contamination or analytical problems may be suspected). Sfax is on the lower side of
217 the IAEA central Mediterranean dataset, which is consistent with its southern
218 location. C-14 and tritium data are averaged using a polynomial function. The curves
219 in Figure 4a and 4b provide the basis for model calculations of the theoretical
220 relationships between the concentrations of the different transient tracers in
221 groundwater under various mixing assumptions.

222 Figure 5 compares the groundwater concentrations of F-11, F-12, F-113 and SF₆
223 for all groundwaters with the piston flow (PF) model, i.e. along tubular flow lines from
224 recharge to discharge with no mixing of the flow lines. Each curve (in black)
225 represents the relationship between a given tracer pair for recharge dates going back

226 in time from the sampling date (2010) to the pre-1950s years corresponding to
227 waters beyond the time-scale of the transient tracers. As a variante to this simple
228 piston flow model, we have also calculated the tracer-tracer relationships (blue
229 curves) for the PF model with a typical dispersion coefficient of 10^{-4} cm²/sec along
230 the direction of the flow (PF+DIS). Figure 5 shows that at all sites the groundwater
231 concentrations disagree with both models and are better explained (dotted line) by a
232 simple binary mixing (BM) between “modern” waters (upper right corner) and “old”
233 tracer free waters (lower left corner). The PF and BM curves define the region that
234 should contain all tracer data if no additional process other than mixing affects the
235 tracer concentration (permitted region). In Figure 5b and 5c, most SF₆ and F-11
236 concentrations are somewhat outside the permitted region. As already noted above
237 when comparing the tracer ages (section 3), this indicates a small but significant
238 additional SF₆ component likely due to in-situ production (Harnisch and Eisenhauer,
239 1998; Busenberg and Plummer, 2000; Deeds et al., 2008; Lapworth et al., 2015) as
240 well as some F-11 in-situ degradation (Oster et al., 1996; Shapiro et al., 1997;
241 Höhener et al., 2003).

242 This mixing trend defined by CFC tracer plots is also apparent on the tritium-F12
243 and tritium-radiocarbon diagrams (Fig. 6a and 6b). This latter diagram also suggests
244 that, for the various studied sites, the old water ¹⁴C endmember is in the range 5 –
245 50 pmC, corresponding to radiocarbon ages between one and four radiocarbon half-
246 lifes (approximately 5000 to 20000 years). Radiogenic ⁴He was plotted against these
247 radiocarbon ages (not shown) since one would expect radiogenic ⁴He coming with
248 the old water. However, as already noticed in the above Results section, for all the
249 sites ³He_{ter} and ⁴He_{ter} are very small and do not provide any clear evidence of a

250 correlation with ^{14}C ages. This is probably because the old waters are too shallow to
 251 pick-up significant crustal helium.

252 The fraction of old water present at each site, estimated from the F113 - F12 or
 253 tritium - F12 diagrams, is shown in Fig. 7.

254 Qualitatively, one may say that this factor of dilution by the old waters is an
 255 indication of size of the reservoir, and therefore of the sustainability of groundwater
 256 resource. More quantitatively, the evolution of the tracer concentration C_n at year n
 257 (for a well-mixed deep reservoir) can be deduced from the tracer concentration C_{n-1}
 258 at year $n-1$ by writing the following tracer balance equation:

$$259 \quad AH_n C_n = AH_{n-1} C_{n-1} + [A r (C_{\text{surf}})_n - A w C_{n-1}] \Delta t \quad (1)$$

260 where Δt equals 1 year, r (in m/year) is the water recharge rate and w (in m/year) is
 261 the withdrawal rate (both natural and anthropic). A (in m^2) is the surface area of the
 262 recharge zone, (AH_n) and (AH_{n-1}) are the volume of groundwater at year n and $n-1$ (in
 263 m^3) and $(C_{\text{surf}})_n$ is the tracer concentration in the recharge water of the year n .

264 In a similar way, the time-evolution of the volume of groundwater obeys the
 265 following equation:

$$266 \quad AH_n = AH_{n-1} + (A r - A w) \Delta t \quad (2)$$

267 If one introduces the renewal time τ_n of the groundwater defined by $\tau_n = H_n/r$,
 268 equations (1) and (2) can be rewritten as follows :

$$269 \quad C_n \tau_n = C_{n-1} \tau_{n-1} + \Delta t [(C_{\text{surf}})_n - C_{n-1} w/r] \quad (1')$$

$$270 \quad \tau_n = \tau_{n-1} + \Delta t (1 - w/r) \quad (2')$$

271 Note that for tritium, a radioactive decay is applied to the concentrations every year
 272 (not shown in the above equations).

273 The concentration C_{2010} of each tracer at the year of sampling (2010) is
274 determined by solving equations (1') and (2') as a function of the initial renewal time
275 τ_{init} of the undisturbed reservoir (before the commissioning of the bottling plant) for
276 various w/r . The value of w/r , which is not known precisely, is assumed equal to 1 in
277 natural conditions. For all the sites where groundwater is pumped from a well,
278 different values of w/r between 1 and 10 are tested. Since C_{2010} must be equal to the
279 measured concentration, a value of τ_{init} can be determined for each tracer.
280 Calculations start in 1950 for CFC's with an initial concentration set to zero. For
281 tritium, an additional spin-up phase going from 1900 to 1950 is necessary to allow for
282 the establishment of the natural concentration in the groundwater reservoir. Table 3
283 displays the value of the renewal time at each site calculated for each tracer for $w/r=1$
284 and $w/r=10$. One can see that the impact of the value chosen for w/r remains limited.
285 This unexpected result is due to the fact that tracer infiltration started in the 1950's,
286 that is well before the commissioning of most of the sites (see Table 1); as a
287 consequence, because of the small withdrawal time compared to the tracer infiltration
288 history, the influence of the withdrawal rate has not enough time to really make a
289 strong difference. Tritium-based renewal times are systematically higher than those
290 of F-12 and F-113. For the majority of the studied sites, renewal times are in the
291 range 50-150 years and, as expected, increase to several centuries (and even
292 millenia) for the sites that show the highest dilution by old waters (Janet, Hayet,
293 Sabine, Marwa).

294 The discrepancy between tritium-based and F-12 / F-133-based renewal times
295 indicates that the well-mixed reservoir hypothesis is clearly oversimplified, thus
296 explaining why the renewal time is affected by the temporal shape of the tracer input
297 function. In actuality, the deep reservoirs are most likely characterized by vertical

298 gradients in tracer concentration. Therefore, analysing tracer concentrations at
299 various depth as well as monitoring tracer concentrations in the mineral waters as a
300 function of time would be very helpful to get a better view of the actual characteristics
301 of groundwater reservoir at each site.

302

303 **5. Conclusion**

304

305 We have analysed anthropogenic tracers (tritium/helium-3, SF₆, CFCs and
306 radiocarbon) in eleven mineral waters of northern and central Tunisia.

307 The analysis of the tracer results show that SF₆ and F-11 are not entirely reliable
308 due to an additional SF₆ component likely originating from in-situ production and a
309 slight but significant F-11 loss attributed to in-situ degradation. All carbon-14 values
310 are well below the natural modern value clearly showing the influence of the ¹⁴C
311 dilution by dead Dissolved Inorganic Carbon. Therefore, the tracer analysis focussed
312 mainly on tritium, F-12 and F-113.

313 Tracer-tracer plots indicate that the analysed groundwaters are a mixture of
314 “modern” rainwater with older waters of pre-1950s ages, which constitute the main
315 groundwater reservoir. ¹⁴C data suggest that the age of these old waters is of the
316 order of radiocarbon half-life or more.

317 The degree of dilution by these old waters is a qualitative indication of size of the
318 reservoir, and therefore of the sustainability of groundwater resource. More
319 quantitatively, the renewal time of each mineral groundwater was estimated using a
320 well-mixed reservoir hypothesis. Most of the studied sites have groundwater renewal
321 times in range from 50-150 years. For the sites where tracer concentrations are the
322 most diluted by old waters, this value increase to several centuries. However one

323 observes some serious discrepancies between tritium based and F-12 / F-133 based
324 results, clearly showing that the well-mixed reservoir hypothesis is oversimplified and
325 calling for additional tracer data and a better resolution of well screens to define the
326 vertical gradients in tracer concentration in the various reservoirs.

327

328 **6. Acknowledgments**

329

330 The authors gratefully acknowledge the helpful contribution of the Office du
331 Thermalisme (Tunis). We also thank the director and technical staff of the mineral
332 water bottling plants for their kindness and assistance during sampling.

333

334 **Appendix A. Geological setting**

335

336 The Tunisian mineral waters are found in various geological domains, trapped in
337 the Jurassic, Upper Cretaceous and Eocene limestone reservoirs as well as the Mio-
338 Pliocene detrital reservoirs.

339 The Marwa mineral waters are captured by an inclined borehole, upstream of Ain
340 el Hammam natural spring. The latter was captured by the Romans via galleries. The
341 Upper Cretaceous fractured and karstified carbonate aquifer forms a large NE-SW
342 synclinal structure affected by faults in the same direction. The centre of the structure
343 is occupied by Paleocene marls providing partial protection of the aquifer against
344 pollution. The aquifer is supplied by infiltration of precipitation waters through
345 widespread carbonates outcropping and forming the Antra and El Hara massifs.

346 Crystalline and Aqualine mineral waters are captured in the Jurassic limestones
347 by two deep drillings of 187 and 96 m respectively, both located to the NW side of the
348 Zaghouan massif. The waters are supplied by infiltration of precipitation in the

349 Zaghouan massif affected by numerous faults: the Zaghouan fault on the SE side
350 and by smaller faults on the NW side (Turki, 1985). The underground flows of
351 Jurassic aquifers waters are oriented towards the NW (mineral water catchment
352 area) and the SE of the Zaghouan massif (Zeriba thermal springs).

353 The Ain Garci mineral waters are captured by a gallery dug in the Eocene
354 limestones. They are probably mixed with the ascending waters of the upper
355 Cretaceous aquifers (Campanian and Cenomanian-Turonian limestones). The
356 physical-chemical characteristics of the mineral waters suggest a deep supply in
357 relation to volcanic rocks (basalt alkaline) associated with the Cenomanian-Turonian
358 carbonates recorded in Jebel Fadhloun and jebel Abid (Raaf and Althuis, 1952;
359 Laaridhi-Ouazaa, 1994). Ain Garci mineral waters show the highest radioactivity,
360 confirming the influence of volcanic rocks (Ben Belgacem, 2011).

361 The mineral water Safia (Ain Mizeb) is captured by a recent gallery in continuity
362 with a Roman gallery and also by drillings (Ain Ksiba). Ain Mizeb is located about 50
363 km south of El Kef and 800 m above sea level. The aquifer is housed in the Eocene
364 limestones of Sra Ouertène (Jellouli). It is a vast limestone plateau resting on the
365 phosphatic layers and covered in places by marls and lumachelles. This plateau is
366 affected by numerous faults and the source (Ain Mizeb) is associated with a fault
367 bringing the Eocene limestone sediments into contact with the marls. The drilling
368 (SO12) capturing Ain Ksiba is located on the edge of the collapsed part of the massif
369 of Sra Ouertene.

370 The mineral water Dima is recovered by a drilling upstream of the Ain M'rada at
371 the level of the wadi Lassoued syncline. This structure is formed by the Eocene
372 limestones and the central part is occupied by the Upper Eocene-Oligocene
373 sediments. It is affected by a series of oblique faults, the most important of which is

374 that of Ain Sassi. This structure constitutes an important hydraulic unit from which
375 emerges several sources: Ain Sassi, Ain Badi and Ain M'rada along the faults. The
376 Eocene limestones constitute the Dima mineral water aquifer. The direction flow of
377 groundwater is SW-NE, so water capture is located in the upstream part of the
378 aquifer.

379 Mineral waters of Fourat, Janet, Sabrine and Hayet are captured by drillings in the
380 Miocene detrital Formation: the water table of Janet aquifer is tapped by a 360 m
381 deep drilling intersecting the Mio-Pliocene detrital Formation near Haffouz (Kairouan)
382 which is in direct contact with Eocene limestone formations.

383 The Fourat mineral water comes from a source located at Ksar Lemsa in the
384 delegation of Oueslatia. The mineral water of Fourat is captured by a deep drilling
385 crossing the Mio-Pliocene formations which are in direct contact with the Eocene
386 limestone.

387 Sabrine waters are captured by a 154 m deep drilling in the southern part of the
388 Chougafia aquifer. It is trapped in a synclinal basin, the core of which is formed by
389 the Mio-Pliocene siliceous sands and is fed by the reliefs surrounding the structure.
390 The water flow of this aquifer is directed SW-NE (Farid et al., 2015) and the drilling,
391 collecting the mineral water is located in the upstream part of the aquifer.

392 Hayet mineral waters are captured by a 226 m deep drilling located at Baten El
393 Ghazel in the delegation of Jelma, 45 km away from Sidi Bouzid. The aquifer is
394 housed in the Miocene sandstone and sealed by marls. Water supply through
395 infiltration occurs throughout sandstones outcropping on the flanks of jebels Labeidh
396 and M'Rihla.

397

398 **7. References :**

399

400 Aeschbach-Hertig, W., Peeters, F., Beyerle, U., Kipfer, R., 1999. Interpretation of
401 dissolved atmospheric noble gases in natural waters. *Water Resour. Res.*, 35,
402 2779-2792.

403 Ambach W, Dansgaard W, Eisner H, Mollner J., 1968. The altitude effect on the
404 isotopic composition of precipitation and glacier ice in the Alps: *Tellus* 20, 595-
405 600.

406 Ayraud, V., Aquilina, L., Labasque, T., Pauwels, H., Molenat, J., Pierson-Wickmann,
407 A.C., Durand, V., Bour, O., Tarits, C., Le Corre, P., Fourre, E., Mérot, P., Davy,
408 P., 2008. Compartmentalization of physical and chemical properties in hard rock
409 aquifers deduced from chemical and groundwater age analyses. *Appl. Geochem.*
410 23, 2686–2707.

411 Battle-Aguilar, J., Banks, E.W., Batelaan, O., Kipfer, R., Brennwald, M.S., Cook,
412 P.G., 2017. Groundwater residence time and aquifer recharge in multilayered
413 semi-confined and faulted aquifer systems using environmental tracers. *J. Hydrol.*
414 546, 150-165.

415 Baudron, P., Barbecot, F., Gillon, M., Arostegui, J.L.G., Travi, Y., Leduc, C., Gomariz
416 Castillo, F., Martinnez-Vicente, D., 2013. Assessing groundwater residence time
417 in a highly anthropized unconfined aquifer using bomb peak ^{14}C and
418 reconstructed irrigation ^3H . *Radiocarbon* 55, 993-1006.

419 Ben Belgacem, S., 2011. Les activités alpha et bêta globales dans l'eau minérale
420 tunisienne. PFE Chimie Industrielle INSA Tunis, 61 pp.

- 421 Beyerle, U., Aeschbach-Hertig, W., Hofer, M., Imboden, D.M., Baur, H., Kipfer, R.,
422 1999. Infiltration of river water to a shallow aquifer investigated with $^3\text{H}/^3\text{He}$, noble
423 gases and CFCs. *J. Hydrol.* 220, 169–185.
- 424 Bullister, J.L., 2011. Atmospheric CFC-11, CFC-12, CFC-113, CCl_4 and SF_6
425 Histories. http://cdiac.ornl.gov/ftp/oceans/CFC_ATM_Hist/. Carbon Dioxide
426 Information Analysis Center, Oak Ridge National Laboratory, US Department of
427 Energy, Oak Ridge, Tennessee.doi: 10.3334/CDIAC/otg.CFC_Hist.
- 428 Busenberg, E. and Plummer, N.L., 2000. Dating Young Groundwater with Sulfur
429 Hexafluoride: Natural and Anthropogenic Sources of Sulfur Hexafluoride, *Water*
430 *Resour. Res.* 36 (10), 3011-3030.
- 431 Busenberg, E., Plummer, L.N., 1992. Use of chlorofluorocarbons (CCl_3F and CCl_2F_2)
432 as hydrologic tracers and age dating tools: the alluvium and terrace system of
433 central Oklahoma. *Water Resour. Res.* 28, 2257–2283.
- 434 Busenberg, E., Plummer, L.N., 2000. Dating young groundwater with sulfur
435 hexafluoride: natural and anthropogenic sources of sulfur hexafluoride. *Water*
436 *Resour. Res.* 36, 3011–3030.
- 437 Celle-Jeanton, H., Zouari, K., Travi, Y., Daoud, A., 2001. Isotopic characterisation of
438 the precipitation in Tunisia. Variations of the stable isotope compositions of rainfall
439 events related to the origin of air masses. *Compte-rendus de l'Académie des*
440 *Sciences, série IIa*, 333, 625-631.
- 441 Clark, I. and Fritz, P., 1997. *Environmental isotopes in hydrogeology*. Lewis
442 Publishers, CRC Press, New York, 331pp.

- 443 Cook, P.G., Solomon, D.K., 1995. Transport of trace gases to the water table:
444 Implications for groundwater dating with chlorofluorocarbons and krypton-85.
445 Water Resour. Res. 31, 263–270.
- 446 Corcho Alvarado, J.A., Purtschert, R., Hinsby, K., Troldborg, L., Hofer, M., Kipfer, R.,
447 Aeschbach-Hertig, W., Arno-Synal H., 2005. ^{36}Cl in modern groundwater dated by
448 a multi-tracer approach ($^3\text{H}/^3\text{He}$, SF_6 , CFC-12 and ^{85}Kr): a case study in
449 quaternary sand aquifers in the Odense Pilot River Basin, Denmark. Appl.
450 Geochem. 20, 599-609.
- 451 Corcho Alvarado, J.A., Purtschert, R., Barbecot, F., Chabault, C., Rueedi, J.,
452 Schneider, V., Aeschbach-Hertig, W., Kipfer, R. and Loosli, H. H., 2007.
453 Constraining the age distribution of highly mixed groundwater using ^{39}Ar : A
454 multiple environmental tracer ($^3\text{H}/^3\text{He}$, ^{85}Kr , ^{39}Ar and ^{14}C) study in the
455 semiconfined Fontainebleau Sands Aquifer (France). Water Resour. Res. 43,
456 W03427, doi:10.1029/2006WR005096.
- 457 Craig, H., 1961. Isotopic variation in meteoric water. Science 133, 1702-1703.
- 458 Darling, W.G., Goody D.C., MacDonald A.M., Morris B.L., 2012. The practicalities of
459 using CFCs and SF_6 for groundwater dating and tracing. Appl. Geochem. 27,
460 1688-1697.
- 461 Deeds, D.A., Vollmer, M.K., Kulongoski, J.T., Miller, B.R., Mühle, J., Harth, C.M.,
462 Izbicki, J.A., Hilton, D.R. and Weiss, R.F., 2008. Evidence for Crustal Degassing
463 of CF_4 and SF_6 in Mojave Desert Groundwaters, Geochim. Cosmochim. Acta 72,
464 999-1013.
- 465 Delbart, C., Barbecot, F., Valdes, D., Tognelli, A., Fourné, E., Purtschert, R.,
466 Couchoux, L., Jean-Baptiste, P., 2014. Investigation of young water inflow in karst

- 467 aquifers using SF₆-CFC-³H/He-⁸⁵Kr-³⁹Ar and stable isotope components. Appl.
468 Geochem. 50, 164-176.
- 469 Farid, I., Zouari, K., Rigane, A., Beji, R., 2015. Origin of the groundwater salinity and
470 geochemical processes in detrital and carbonate aquifers: Case of Chougafiya
471 basin (Central Tunisia). J. Hydrol. 530, 508-532.
- 472 Fourré E., Di Napoli, R., Aiuppa, A., Parello, F., Gaubi, E., Jean-Baptiste, P., Allard,
473 P., Calabrese, S., Ben Mammou, A., 2011. Regional variations in the chemical and
474 helium-carbon isotope composition of geothermal waters across Tunisia.
475 Chemical Geology 288, 67-85.
- 476 Frija, A., Chebil, A., Speelman, S., Faysse, N., 2014. A critical assessment of
477 groundwater governance in Tunisia. Water Policy 16, 358-373.
- 478 Gat, J.R. and Carmi, I., 1970. Evolution of the isotopic composition of atmospheric
479 waters in Mediterranean Sea area, J. Geophys. Res. 75, 3039-3048.
- 480 Goody, D.C., Darling, W.G., Abesser, C., Lapworth, D.J., 2006. Using
481 chlorofluorocarbons (CFCs) and sulphur hexafluoride (SF₆) to characterise
482 groundwater movement and residence time in a lowland Chalk catchment. J.
483 Hydrol. 330, 44-52.
- 484 Harnisch, J. and Eisenhauer, A., 1998. Natural CF₄ and SF₆ on Earth. Geophys. Res.
485 Lett. 25 (13), 2401-2404.
- 486 Han, L.F., Plummer, L.N., 2016. A review of single-sample-based models and other
487 approaches for radiocarbon dating of dissolved inorganic carbon in groundwater.
488 Earth Science Reviews 152, 119-142.
- 489 Höhener, P., Werner, D., Balsiger, C., Pasteris, G., 2003. Worldwide occurrence and
490 fate of chlorofluorocarbons in groundwater. Water Resour. Res. 33, 1-33.

- 491 Jean-Baptiste, P., Mantsi, F., Dapoigny, A., Stievenard, M., 1992. Design and
492 performance of a mass spectrometric facility for measuring helium isotopes in
493 natural waters and for low-level tritium determination by the ^3He ingrowth method.
494 Int. J. Radiat. Appl. Instrum. 43, 881-891.
- 495 Jean-Baptiste, P., Fourré, E., Dapoigny, A., Baumier, D., Baglan, N., Alanic, G.,
496 2010. ^3He mass spectrometry for very low-level measurement of organic tritium
497 in environmental samples. J. Environ. Rad., 101, 185-190.
- 498 Kralik, M., Humer, F., Fank, J., Harum, T., Klammler, G., Goody, D., Sültenfuß, J.,
499 Gerber, C., Purtschert, R. 2014. Using $^{18}\text{O}/^2\text{H}$, $^3\text{H}/^3\text{He}$, ^{85}Kr and CFCs to
500 determine mean residence times and water origin in the Grazer and Leibnitzer
501 Feld groundwater bodies (Austria). Appl. Geochem. 50, 150-163.
- 502 Laaridhi-Ouazaa, N., 1994. Etude minéralogique et géochimique des épisodes
503 magmatiques mésozoïques et miocènes de la Tunisie. PhD Thesis, Univ. Tunis II,
504 457 pp.
- 505 Labasque, T., Ayraud, V., Aquilina, L., Le Corre, P., 2006. Dosage des composés
506 chlorofluorocarbonés et du tétrachlorure de carbone dans les eaux souterraines.
507 Application à la datation des eaux. Editions Géosciences Coll Cahiers
508 Techniques. ISBN:2-914375-38-7.
- 509 Lapworth, D.J., MacDonald, A.M., Krishan, G., Rao, M.S., Goody, D.C. and Darling,
510 W.G., 2015. Groundwater recharge and age-depth profiles of intensively exploited
511 groundwater resources in northwest India, Geophys. Res. Lett., 42, 7554–7562,
512 doi:10.1002/2015GL065798.
- 513 Lucas, L.L., Unterweger, M.P., 2000. Comprehensive review and critical evaluation of
514 the half-life of tritium. J. Res. Natl. Inst. Stand. Technol. 105, 541-549.

- 515 Massmann, G., Sültenfuß, J., Dünnebier, U., Knappe, A., Taute, T., Pekdeger, A.,
516 2008. Investigation of groundwater residence times during bank filtration in Berlin:
517 a multi-tracer approach. *Hydrol. Process.* 22, 788–801.
- 518 Mayer, A., Sültenfuß, J., Travi, Y., Rebeix, R., Purtschert, R., Claude, C., Le Gal La
519 Salle, C., Miche, H., Conchetto, E., 2014. A multi-tracer study of groundwater
520 origin and transit-time in the aquifers of the Venice region (Italy). *Appl. Geochem.*
521 50, 177-198.
- 522 Nydal, R., and K. Lövseth. 1996. Carbon-14 Measurements in Atmospheric CO₂ from
523 Northern and Southern Hemisphere Sites, 1962-1993. ORNL/CDIAC-93, NDP-
524 057. Carbon Dioxide Information Analysis Center, Oak Ridge National Laboratory,
525 Oak Ridge, Tennessee. 67 pp. doi: 10.3334/CDIAC/atg.ndp057
- 526 Oster, H., Sonntag, C., Munnich, K.O., 1996. Groundwater age dating with
527 chlorofluoro-carbons. *Water Resour. Res.* 32 (10), 2989-3001.
- 528 Plummer, L.N., Busenberg, E., Böhlke, J.K., Nelms, D.L., Michel, R.L., Schlosser, P.,
529 2001. Groundwater residence times in Shenandoah National Park, Blue Ridge
530 Mountains, Virginia, USA: a multi-tracer approach. *Chemical Geology* 179, 93-
531 111.
- 532 Plummer, L.N. and Glynn, P.D., 2013. Radiocarbon dating in groundwater systems.
533 In: *Isotope methods for dating old groundwater*, International Atomic Energy
534 Agency, Vienna, STI/PUB/1587, Chapter 4, 33-89.
- 535 Poreda, R.J., Cerling, T.E. and Solomon, D.K., 1988. Tritium and helium isotopes as
536 hydrologic tracers in a shallow unconfined aquifer. *J. Hydrol.*, 103, 1-9.

- 537 Raaf, J.F.M. and Althuis, S.P., 1952. Présence d'ophites spilitiques dans le Crétacé
538 des environs d'Enfidaville. 19th International Geological Congress, Algiers, 2^d Ser.
539 Tunisia 6, 127-137.
- 540 Schlosser, P., Stute, M., Dörr, H., Sonntag, C. and Münnich, K.O., 1988. Tritium/³He
541 dating of shallow groundwater. Earth Planet. Sci. Lett., 89, 353-362.
- 542 Shapiro, S.D., Schlosser, P., Smethie, W.M., Stute, M., 1997. The use of H-3 and
543 tritogenic He-3 to determine CFC degradation and vertical mixing rates in
544 Framvaren Fjord, Norway. Marine Chemistry 59 (1-2), 141-157.
- 545 Siegenthaler, U. and Oeschger, H., 1980. Correlation of ¹⁸O in precipitation with
546 temperature and altitude, Nature 285, 314-317.
- 547 Solomon, D.K. and Sudicky, E.A., 1991. Tritium and helium-3 isotope ratios for direct
548 estimation of spatial variations in groundwater recharge. Water Resour. Res.,
549 27(9), 2309-2319.
- 550 Solomon, D.K., Schiff, S.L., Poreda, R.J. and Clarke, W.B., 1993. A validation of the
551 ³H/³He method for determining groundwater recharge. Water Resour. Res., 29(9),
552 2951-2962.
- 553 Solomon D.K., Genereux D.P., Plummer L.N., Busenberg E., 2010. Testing mixing
554 models of old and young groundwater in a tropical lowland rain forest with
555 environmental tracers. Water Resour. Res. 46, W04518,
556 doi:10.1029/2009WR008341.
- 557 Stewart, M.K., 2012. A 40-year record of carbon-14 and tritium in the Christchurch
558 groundwater system, New Zealand: dating of young samples with carbon-14. J.
559 Hydrol. 430, 50-68.

560 Stute, M., Deák, J., Révész, K., Böhlke, J.K., Deseö, E., Weppernig, R., Schlosser,
561 P., 1997. Tritium/³He dating of river infiltration: an example from the Danube in
562 the Szigetköz Area, Hungary. *Groundwater* 35 (5), 905–911.

563 Suckow, A., 2014. The age of groundwater – Definitions, models and why we do not
564 need this term. *Appl. Geochem.* 50, 222-230.

565 Szabo, Z., Rice, D.E., Plummer, L.N., Busenberg, E., Drenkard, S., Schlosser, P.,
566 1996. Age dating of shallow groundwater with chlorofluorocarbons, tritium/helium-
567 3, and flow path analysis, southern New Jersey coastal plain. *Water Resour. Res.*
568 32 (4), 1023–1038.

569 Thompson, G.M. and Hayes J.M., 1979. Trichloromethane in groundwater: A
570 possible tracer and indicator of groundwater age. *Water Resour. Res.*, 15, 546-
571 554.

572 Turki M.M., 1985. Polycinématique et contrôle sédimentaire associé sur la cicatrice
573 Zaghuan- Nebhana. PhD Thesis, Univ. Tunis. C. ST-INRST Ed., 7, 252 pp.

574

575

576

577 **Figure captions**

578

579 Fig.1 : Map of Northern and Central Tunisia showing the location of the groundwater
580 sampling sites.

581

582 Fig.2 : Comparison of the stable isotopic composition of precipitation with the isotopic
583 composition of the groundwaters. Tunis and Sfax Local Meteoric Water Lines (dotted
584 lines) are from Celle-Jeanton et al. (2001). The Global Meteoric Water Line (GMWL)
585 and Mediterranean Meteoric Water Line (MMWL) are from Craig (1961) and Gat &
586 Carmi (1970), respectively.

587

588 Fig.3 : Tracer ages comparison : ^3H - ^3He (light blue), F-11 (red), F-12 (yellow), F-113
589 (green), SF_6 (dark blue)

590

591 Fig.4 : Atmospheric concentration of the transient tracers for the northern hemisphere
592 as a function of time. CFC and SF_6 curves (a) are from Bullister (2011) and ^{14}C data
593 are from Nydal & Lövseth (1996). Tritium content of rainwater in Tunisia (b) was
594 constructed using all historical measurements from Central Mediterranean stations in
595 the IAEA Global Network of Isotopes in Precipitation database (at
596 <https://nucleus.iaea.org/wiser/gnip.php>), including the times-series of tritium in
597 rainwater for Tunis and Sfax.

598

599 Fig.5 : CFC and SF_6 tracer plots showing F-113 versus F-12 (a), SF_6 versus F-12 (b)
600 and F-11 versus F-12 (c). The black and blue curves correspond to the PF model
601 and the PF model + dispersion respectively (see text). Numbers are travel times (in

602 year) in the PF model. The dotted line represents the mixing between a recharge
603 water of the year 2010 (upper right corner) and an old water endmember with zero
604 tracer concentration (lower left corner).

605

606 Fig.6 : (a) ^3H versus F-12. The black and blue curves correspond to the PF model
607 and the PF model + dispersion respectively (see text). Tritium values prior to 2010
608 are decay-corrected using a tritium half-life of 4500 d (Lucas and Unterweger, 2000).
609 Dotted curve represent mixing between old waters and a recharge water of the year
610 2010 . (b) ^3H versus ^{14}C (corrected for carbonate dissolution). NB: the initial ^{14}C value
611 of recharge waters, as given by the ^{14}C input function (Fig. 4a), can be modified by
612 interaction of infiltrating water with soil CO_2 from plant root respiration and microbial
613 degradation of soil organic matter. In semi-arid to arid environments however, those
614 biological interactions are minimal (Plummer and Glynn, 2013) so this effect is
615 neglected here.

616

617 Fig.7 : Comparison of the fraction of old water present at each site, estimated from
618 the F113 - F12 and tritium - F12 diagrams.

619

620

621 **Table captions**

622

623 Table 1 : Summary of the main relevant parameters for the sampled sites

624

625 Table 2 : Tracer results. CFCs and SF₆ tracer concentrations have been corrected
626 from excess air as defined by neon data and normalized to sea-level pressure and a
627 common temperature of 15°C to allow the comparison of all sites (note that the
628 uncertainty on CFC and SF₆ ages do not take into account the uncertainty on the air
629 excess correction, mostly because of the lack of knowledge of the exact recharge
630 altitude).

631

632 Table 3 : Estimated groundwater renewal time for the various sites based on tritium,
633 F-12 and F-113 data, assuming a well-mixed reservoir (see text).

Site	Geographic zone	Catchment type	Well depth (m)	Year of commissioning	Altitude of the site (m)	Average temperature (°C)		Average precipitation (mm)			Recharge temperature (°C) (precipitation weighed)	pH	HCO ₃ (mmol/l)
						January	July	January	July	Annual			
Marwa	Bizerte	well	72	1993	300	11,3	25,2	77	3	558	13,1	7,2	4,17
Safia (Ain Mizeb)	El Kef	surface	0	1968	880	7,1	26,5	65	9	509	12,9	7,3	3,87
Safia (Ain Ksiba)	El Kef	well	62	1992	900	7,1	26,5	65	9	509	12,7	7,0	3,71
Dima	El Kef	well	~50	2009	750	7,1	26,5	65	9	509	13,7	7,5	4,04
Cristaline	Zaghouan	well	187	2003	200	9,6	27,0	68	5	496	15,2	7,4	3,79
Aqualine	Zaghouan	well	96	2006	200	9,6	27,0	68	5	496	15,2	7,6	4,40
Ain Gardi	Zaghouan	surface	0	1900	110	9,6	27,0	68	5	496	15,2	6,6	19,84
Sabrine	Kairouan	well	154	1991	106	11,7	29,1	23	5	306	17,6	7,5	3,80
Fourat	Kairouan	well	~150	2003	400	11,7	29,1	23	5	306	16,1	7,2	4,80
Hayet	Kairouan	well	226	1996	420	11,7	29,1	23	5	306	16,0	7,5	2,15
Jannet	Kairouan	well	360	2002	400	11,7	29,1	23	5	306	16,1	7,6	3,75

Table 1

Site	Tritium (TU)	Neon excess (%)	3H-3He age (year)	F-11 (pmol/L)		F-12 (pmol/L)		F-113 (pmol/L)		SF6 (pmol/L)		F-11 age (year)	F-12 age (year)	F-113 age (year)	SF6 age (year)	2-H	18-O	14-C (pmC)	delta 13-C (permil)	14-C corrected (pmC)
Marwa (2009)	1,44 ± 0,13	230,1	34,6 ± 1,4															52,27 ± 0,21	-11,14	56,30
Marwa	1,35 ± 0,05	26,6	23,9 ± 0,6	0,69 ± 0,12	0,549 ± 0,07	0,081 ± 0,01	7,99E-04 ± 1,2E-04	42 ± 2	40 ± 3	32 ± 2	20 ± 2	-35,7	-6,45							
Safia-Ain Mizeb (2009)	3,29 ± 0,15	11,0	10,4 ± 2,4													-49,1	-7,84	55,07 ± 0,19	-11,82	55,90
Safia-Ain Ksiba	3,34 ± 0,06	7,3	9,98 ± 1,1	2,08 ± 0,12	1,320 ± 0,07	0,208 ± 0,01	1,27E-03 ± 1,2E-04	34 ± 2	31 ± 2	25 ± 2	13 ± 2	-49,9	-7,66	58,01 ± 0,22	-12,36	58,01				
Dima	3,03 ± 0,08	50,1	12,9 ± 1,0	1,43 ± 0,12	1,067 ± 0,07	0,176 ± 0,01	1,33E-03 ± 1,2E-04	37 ± 2	34 ± 2	26 ± 2	12 ± 2	-50,5	-7,62	68,72 ± 0,24	-12,22	68,72				
Cristaline	3,10 ± 0,08	34,5	19,8 ± 0,7	1,64 ± 0,12	1,134 ± 0,07	0,165 ± 0,01	1,66E-03 ± 1,2E-04	36 ± 2	33 ± 2	24 ± 2	8 ± 1	-36,3	-6,51	67,93 ± 0,24	-10,47	77,86				
Aqualine	3,16 ± 0,12	31,1	19,5 ± 0,6	1,64 ± 0,12	1,069 ± 0,07	0,166 ± 0,01	1,73E-03 ± 1,2E-04	36 ± 2	34 ± 2	26 ± 2	7 ± 1	-36,0	-6,52	66,43 ± 0,21	-10,57	75,42				
Ain Garci (2009)	0,49 ± 0,04	-0,4														-31,7	-5,65	2,25 ± 0,09	-0,75	36,00
Sabrine	0,23 ± 0,05	10,9	37,1 ± 1,7	0,14 ± 0,12	0,061 ± 0,07	0,034 ± 0,01	1,84E-04 ± 1,2E-04	51 ± 2	56 ± 3	37 ± 2	33 ± 2	-31,6	-5,26	31,30 ± 0,14	-8,50	44,19				
Fourat	2,53 ± 0,05	8,2	26,8 ± 1,0	1,30 ± 0,12	0,894 ± 0,07	0,136 ± 0,01	1,20E-03 ± 1,2E-04	38 ± 2	36 ± 2	28 ± 2	14 ± 2	-38,8	-6,59	60,66 ± 0,20	-11,35	64,13				
Hayet	0,10 ± 0,06	38,8	55,7 ± 17,7	0,25 ± 0,12	0,185 ± 0,07	0,031 ± 0,01	2,33E-04 ± 1,2E-04	48 ± 2	51 ± 3	43 ± 2	31 ± 2	-32,2	-5,10	34,54 ± 0,16	-10,94	37,89				
Jannet	0,12 ± 0,07	16,3	48,1 ± 16,3	0,12 ± 0,12	0,045 ± 0,07	0,025 ± 0,01	3,02E-04 ± 1,2E-04	52 ± 2	58 ± 3	39 ± 2	29 ± 2	-37,2	-6,32	3,62 ± 0,10	-7,49	5,80				

Table 2

Site	Tritium-based renewal time (yr)		F12-based renewal time (yr)		F113-based renewal time (yr)	
	w/r = 1	w/r = 10	w/r = 1	w/r = 10	w/r = 1	w/r = 10
Marwa	329	360	131	215	125	215
Safia-Ain Mizeb	108	n.a	-	-	-	-
Safia-Ain Ksiba	106	186	41	183	38	183
Dima	122	135	57	69	49	61
Cristaline	118	134	52	89	53	90
Aqualine	114	129	57	75	53	72
Ain Garci	950	n.a	-	-	-	-
Sabrina	2100	2100	1320	1390	320	400
Fourat	155	171	72	102	68	100
Hayet	4500	4500	430	470	350	400
Jannet	4100	4100	1800	1800	440	470

Table 3



Figure 1

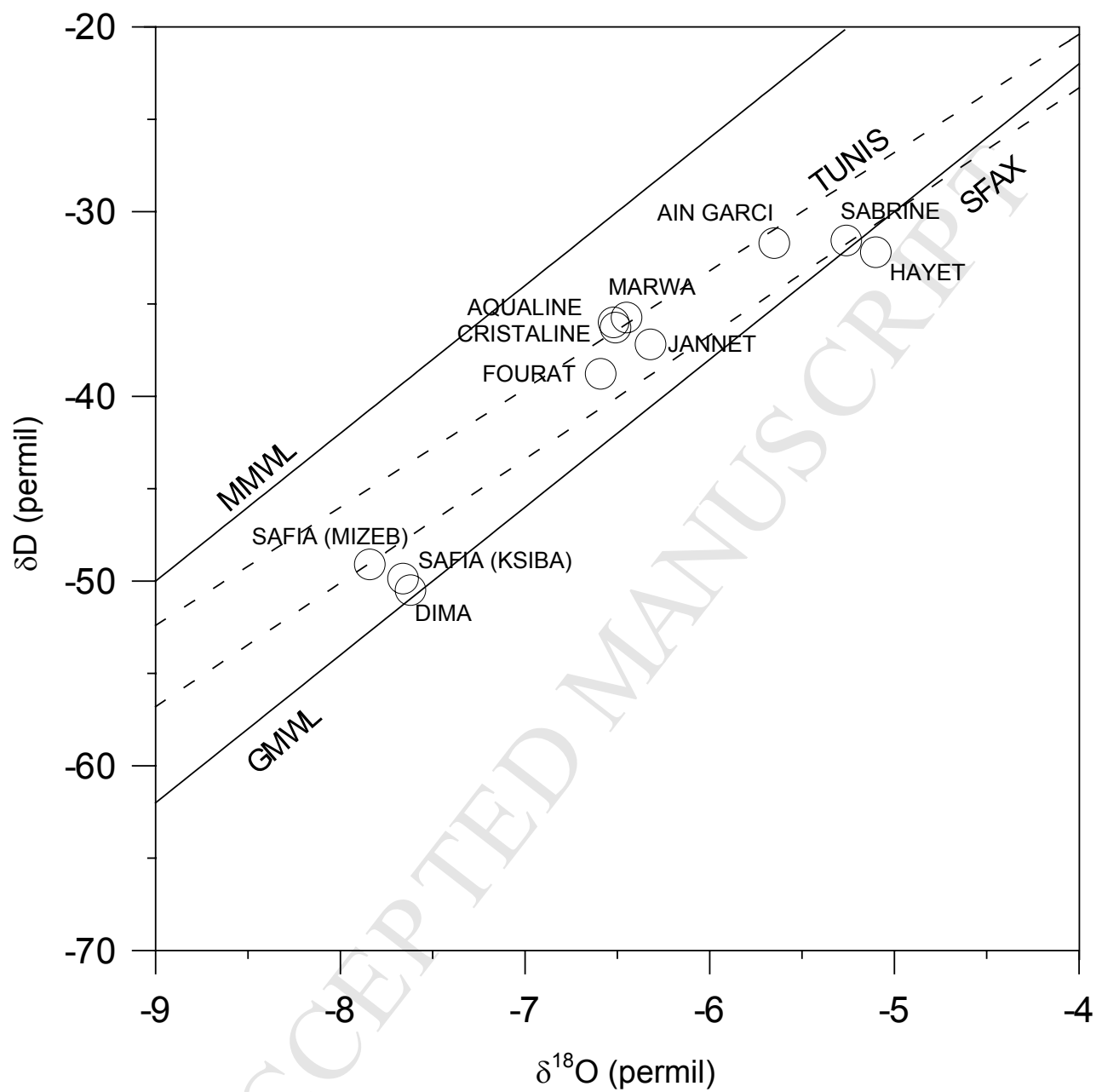


Figure 2

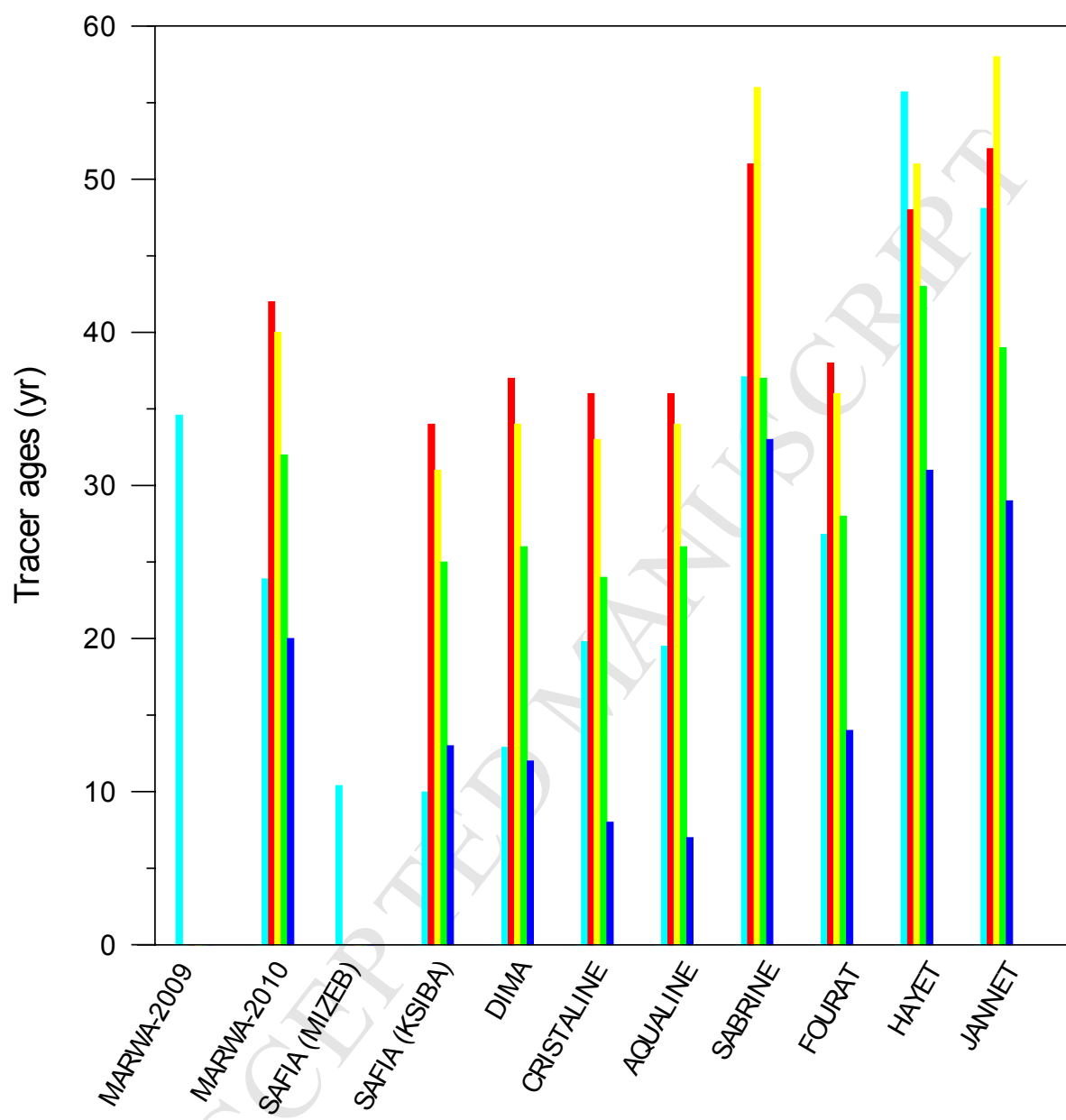


Figure 3

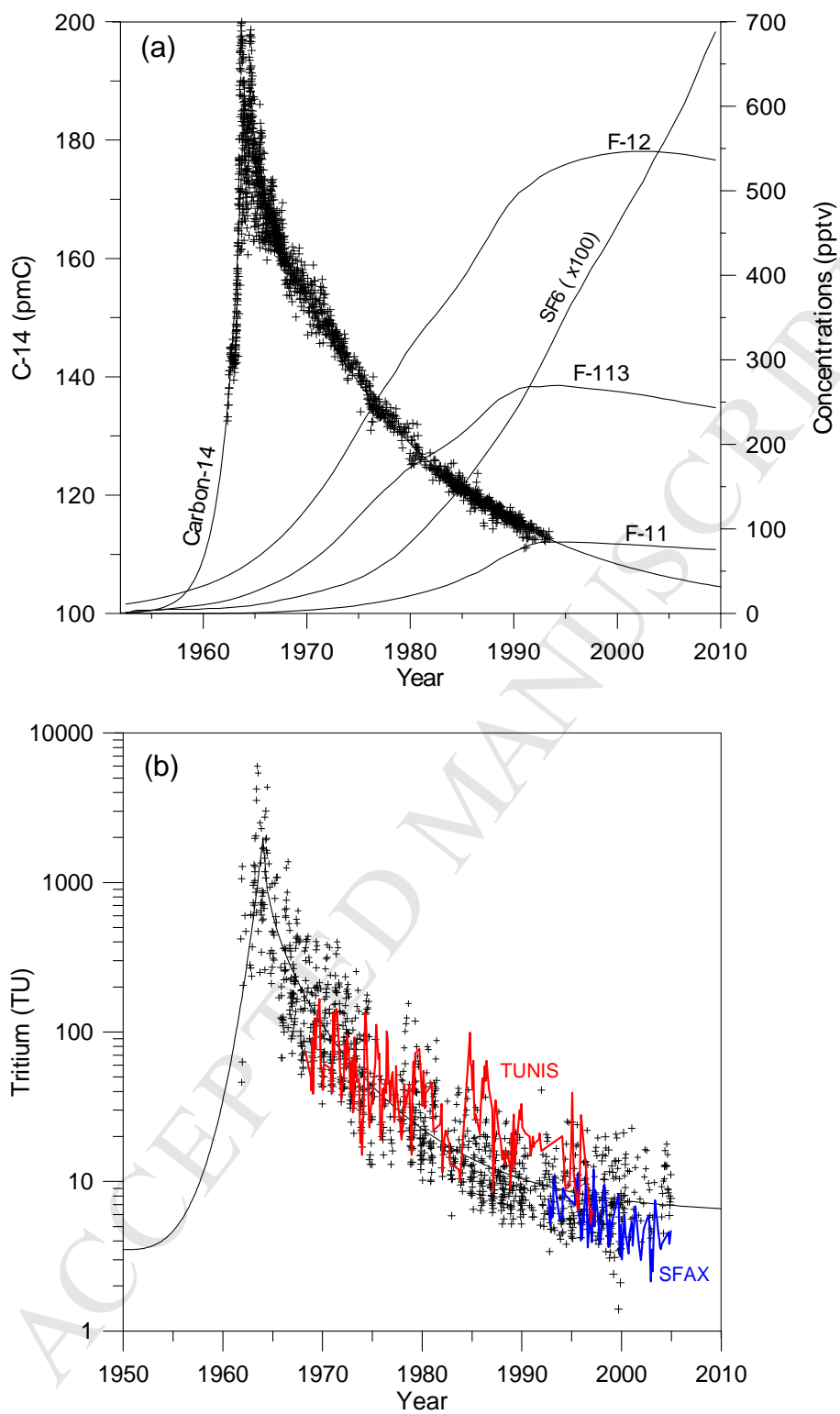


Figure 4

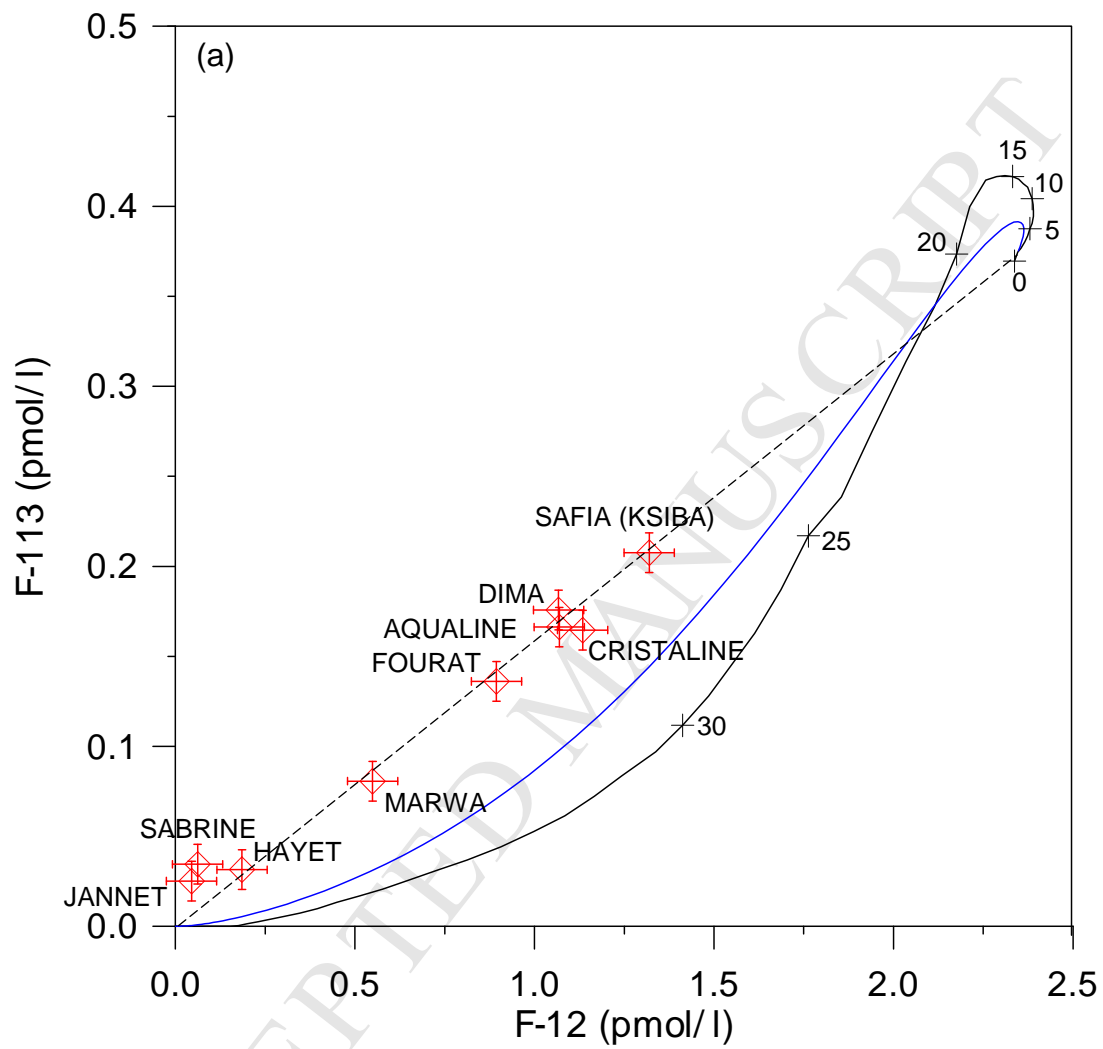


Figure 5a

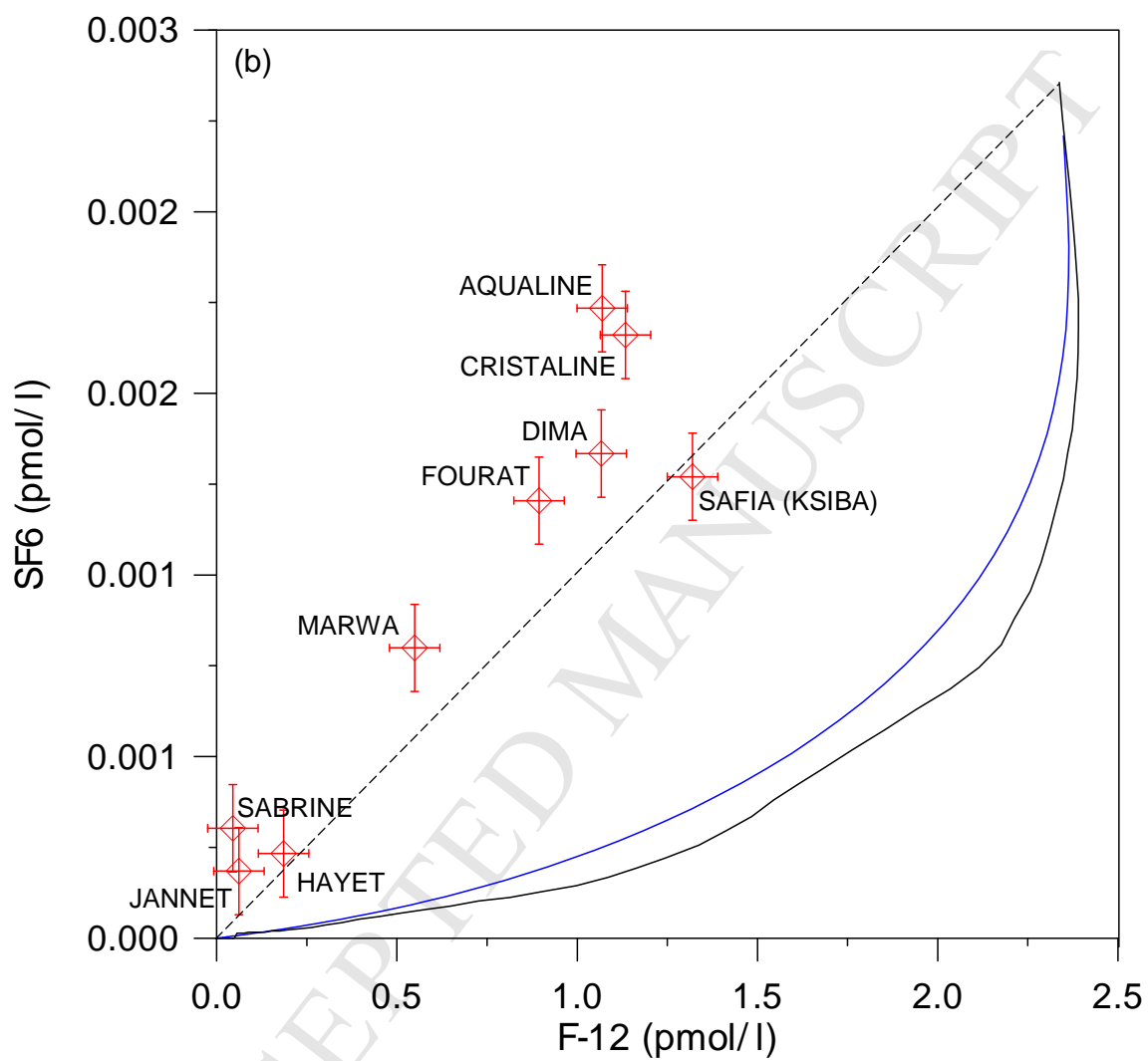


Figure 5b

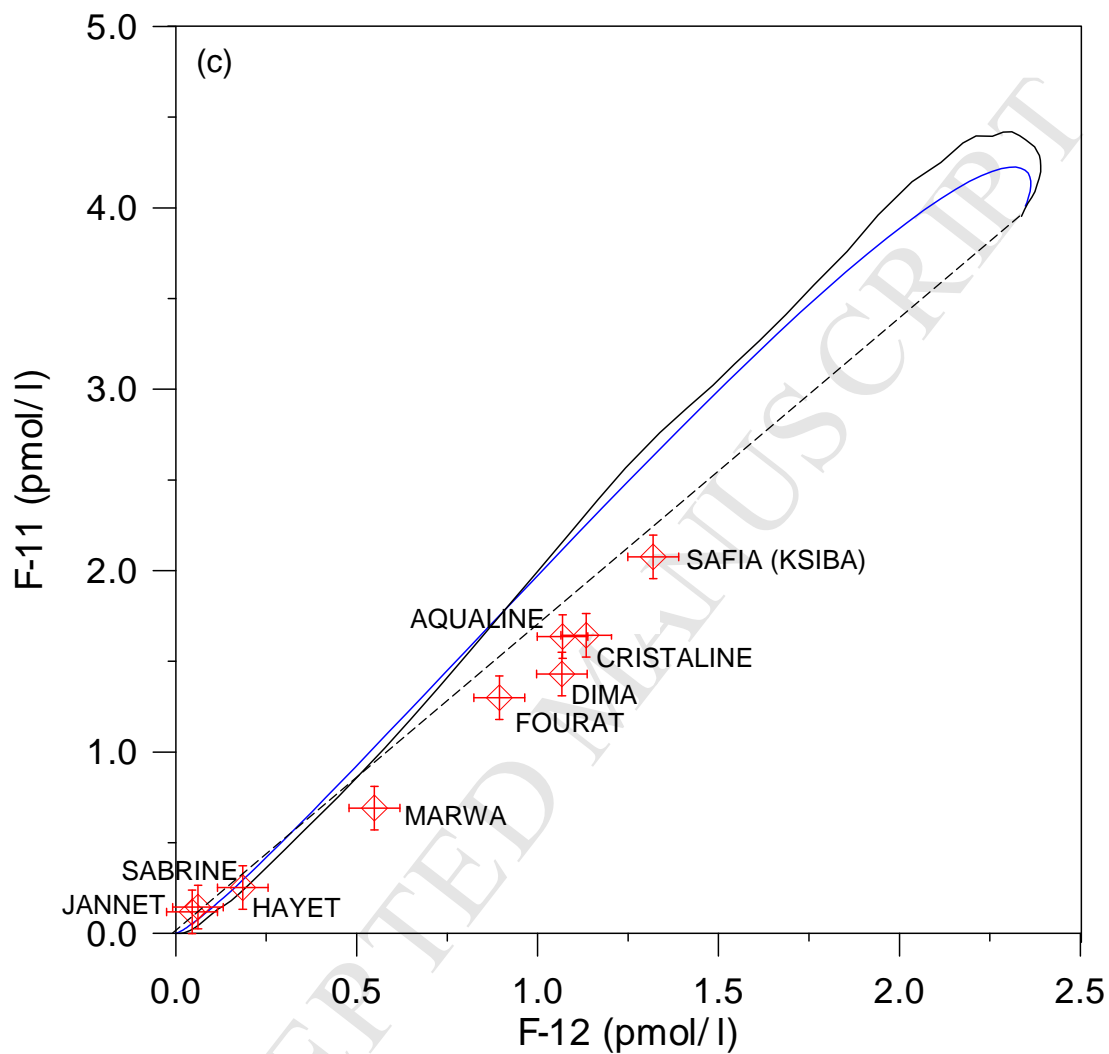


Figure 5c

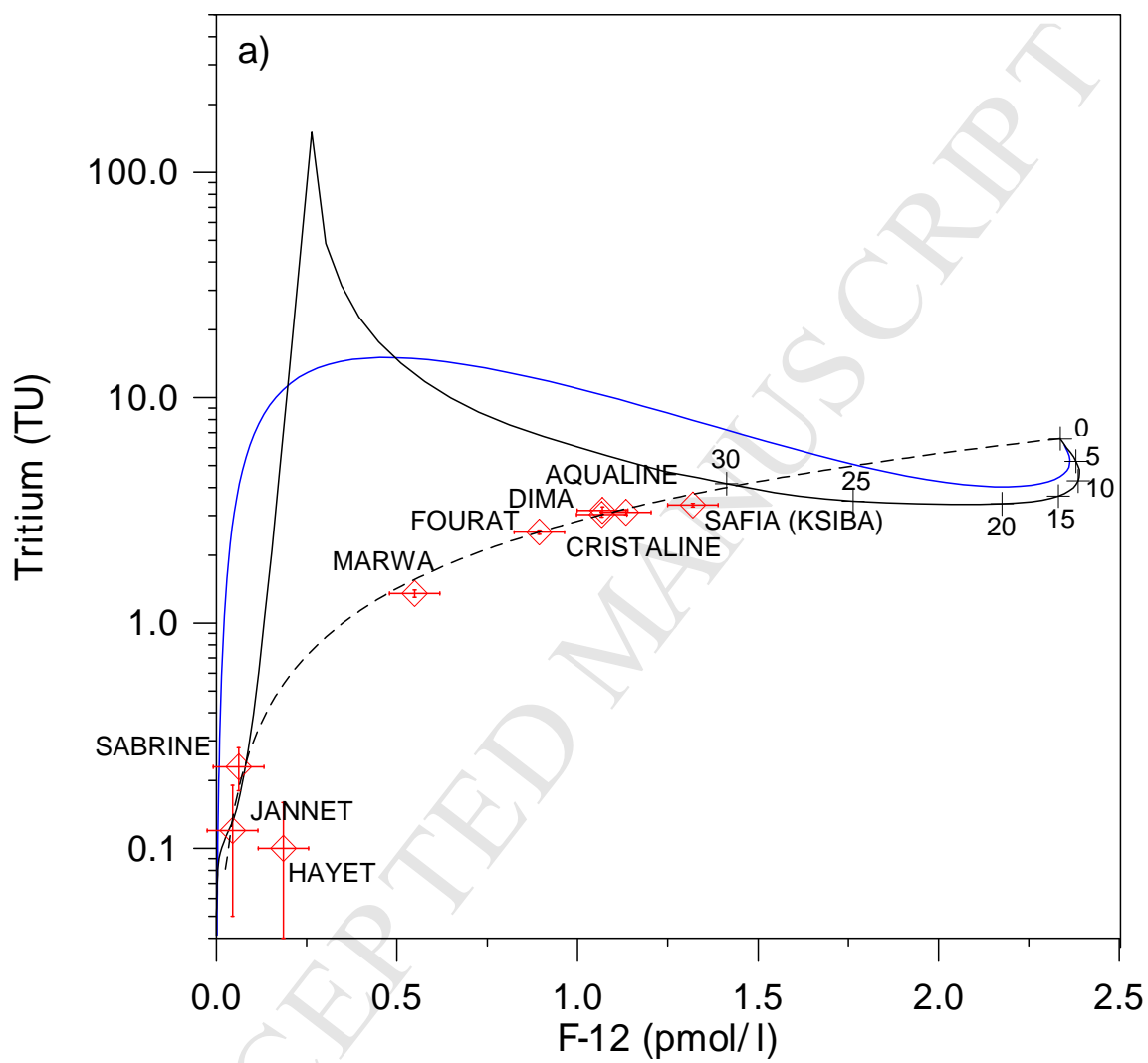


Figure 6a

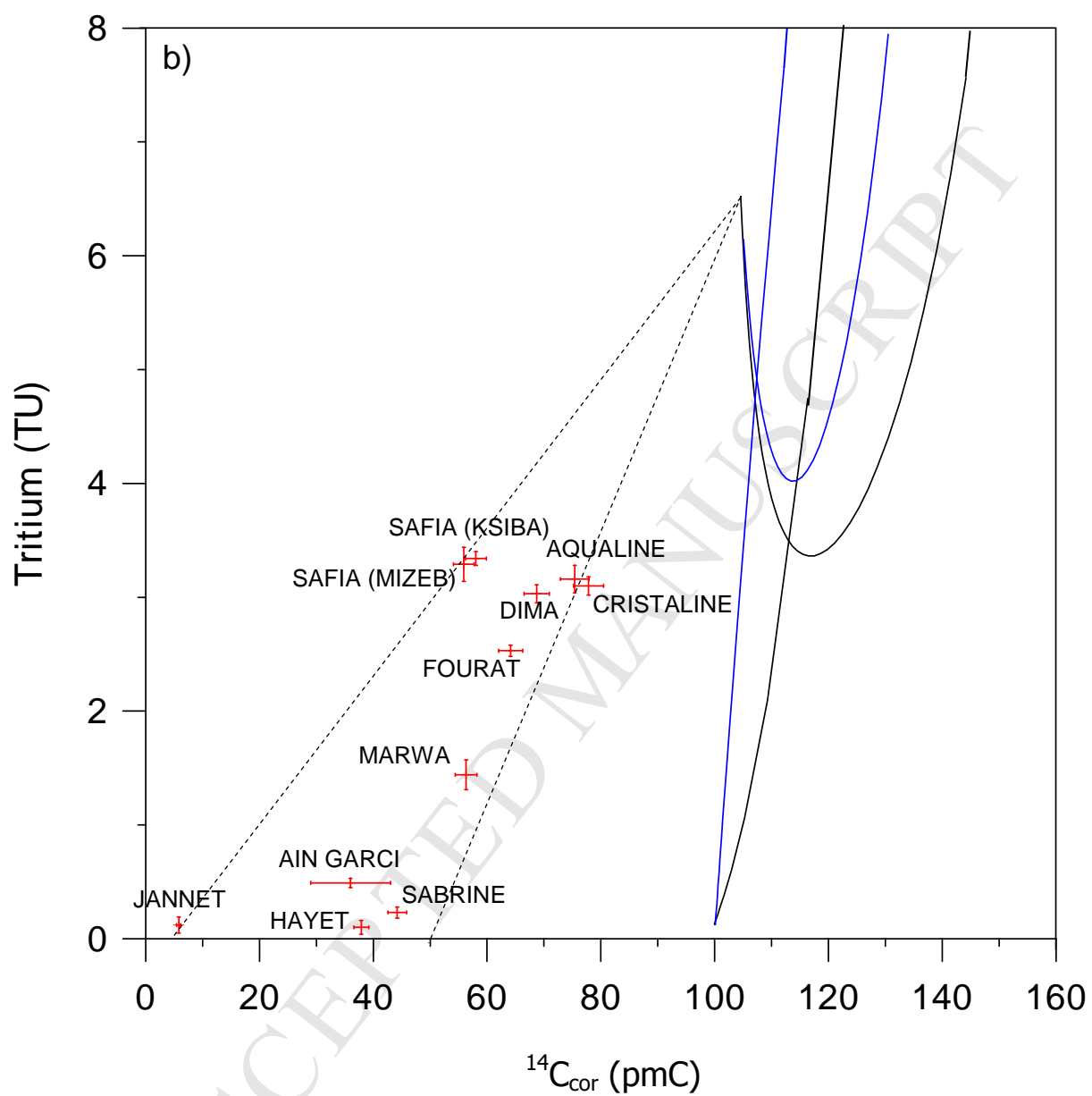


Figure 6b

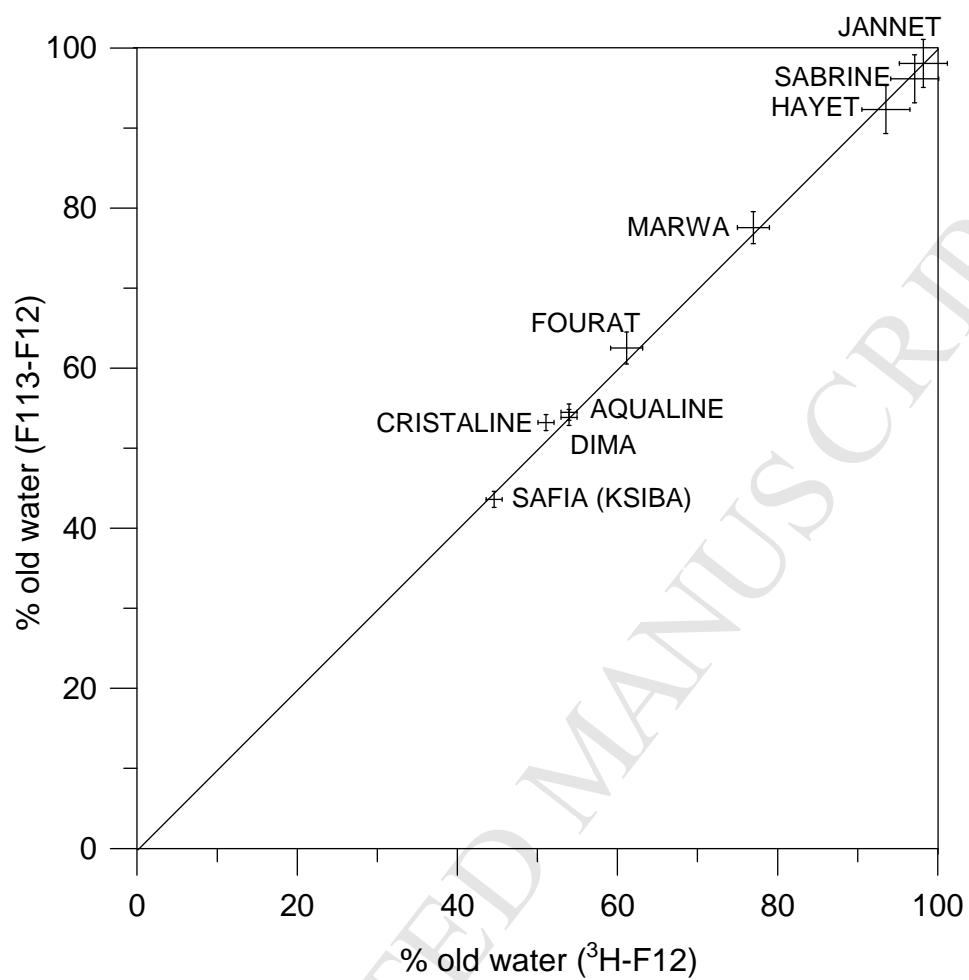


Figure 7

^3H - ^3He , CFCs, SF_6 and ^{14}C were analyzed in commercial mineral groundwaters of Tunisia

All studied groundwaters are a mixture of modern rainwater with old groundwaters

Radiocarbon ages of these old groundwaters are in the range 5000-20000 years

Most groundwaters have renewal times between 50 years and several centuries